J. Phase Equilib. Diffus. (2018) 39:196–203
https://doi.org/10.1007/s11669-018-0621-8

The Isothermal Section of the Zr-Sn-Cu Ternary System at 700 °C

Gaihuan Yuan[1] · Wenbin Luo[2,3] · Yifang Ouyang[3] · Jianlie Liang[2]

Submitted: 24 August 2016 / in revised form: 7 February 2018 / Published online: 23 February 2018

Abstract The isothermal section of the Zr-Sn-Cu ternary system at 700 °C was investigated by using x-ray diffraction, scanning electron microscope and energy dispersive spectroscopy. A new ternary compound τ ($Zr_{25.3}Cu_{66.1}Sn_{8.6}$) was observed in the Cu-rich corner of this system. The previous known ZrCuSn and $ZrCuSn_2$ ternary compound were confirmed.

Keywords phase equilibria · zirconium alloys · Zr-Sn-Cu alloys

1 Introduction

Copper alloys are widely used in electrical industries because of their excellent electrical and thermal conductivities. Additional of Zr and other alloying elements improve the strength of copper alloys.[1,2] Zirconium alloys are widely used as cladding and core structure materials in fuel reactions, due to their low neutron absorbtion cross section, perfect corrosion and creep resistance properties in high pressure and high temperature environment.[3] Tin is a common alloying element in commercial zirconium alloys, since the addition of tin offsets the deterioration of corrosion resistance by nitrogen and improves the creep resistance of alloys.

Development of the HANA serial alloys (Zr-Nb-Cu alloys) indicates that copper has a positive effect on the corrosion resistance of commercial zirconium alloys.[4–7] Since the development of the HANA serial alloys, dilute copper additions have been added to experimental Zr-based alloys to improve their corrosion resistance.[8–14] Among those experimental alloys, Zr-Sn-Cu is an important subsystem. Though no Sn-containing compound has been reported in commercial zirconium alloys, the interaction of tin with Zr and other alloying elements is still vital for understanding phase transformations in commercial Zr-based alloys. For example, the interaction of tin and other alloying elements will change the phase boundary between α-Zr and β-Zr as well as those between α-Zr, β-Zr, and precipitates. Temperatures associated with these boundaries are very important for thermal fabrication.

Most commercial Zr-based alloys are multicomponent. To understand phase transitions in multicomponent alloys, having a thermodynamic description of the alloys by using CALPHAD techniques is both convenient and powerful.[15] Experimental work on binary and ternary phase diagrams provide basic data for the thermodynamic optimization of databases. To benefit the establishment of a thermodynamic description of the Zr-based alloys, this work aims to determine phase equilibria in the Zr-Sn-Cu system.

Subsytems for the Zr-Sn-Cu alloy are the Zr-Cu, Zr-Sn, and Cu-Sn binary systems. In 1990, Aria and Abriata assessed the phase diagram of the Zr-Cu system.[16] According to Aria and Abriata, there are 8 compounds existing in the Zr-Cu system, i.e., Cu_9Zr_2, CuZr, $Cu_{10}Zr_7$, $Cu_{24}Zr_{13}$, Cu_2Zr, Cu_8Zr_3, $Cu_{51}Zr_{14}$, and Cu_5Zr. Later, Zeng et al.[17] optimized this system. Zeng et al.[17] pointed out that Cu_5Zr rather than Cu_9Zr_2 exists in this system.

✉ Jianlie Liang
jianlieliang@126.com

1 State Nuclear Bao Ti Zirconium Industry Company, Baoji 721014, China

2 School of Science, Guangxi University of Nationalities, Nanning 530006, China

3 School of Physical Science and Engineering Technology, Guangxi University, Nanning 530004, China

According to Zeng et al.,[17] the stable phases at 700 °C for the Zr-Cu system are $CuZr_2$, $Cu_{10}Zr_7$, Cu_8Zr_3, $Cu_{51}Zr_{14}$, and Cu_5Zr. In 2010, a thermodynamic assessment of the Zr-Cu system has been carried out by Kang and Jung.[18] Kang and Jung[18] reported that the stable compounds in the Zr-Cu system were Cu_9Zr_2, $Cu_{51}Zr_{14}$, Cu_8Zr_3, Cu_2Zr, $C_{10}Zr_7$, CuZr, Cu_5Zr_8, and $CuZr_2$. Recently, a new experiment work and thermodynamic assessment on the Zr-Cu system were conducted by Liu et al.[19] Experiment work from Liu et al. revealed that Cu_2Zr and Cu_5Zr_8 were not the stable phases. This result is consistent with that in Ref 17. As discussed by Zeng et al.[17], the existence of Cu_5Zr was supported by XRD results on the extracted precipitate,[20] and electron diffraction results on the precipitate in spray-cast Cu-Zr alloys.[21] Recently, results from electron diffraction confirmed that Cu_5Zr was the stable compound in the Zr-Cu system too.[22,23] It shows that the modeling work of the Zr-Cu system by Liu et al.[19] is more reliable than that by Kang and Jung.[18] Summarily, the stable compounds in Zr-Cu system are Cu_5Zr, $Cu_{51}Zr_{14}$, Cu_8Zr_3, $C_{10}Zr_7$, CuZr, and $CuZr_2$. CuZr is a high temperature phase, which decomposes through eutectoid reaction $CuZr \leftrightarrow Cu_{10}Zr_7 + CuZr_2$ at 717.6 °C.[19]

The Cu-Sn phase diagram was experimentally re-investigated by Fütauer et al.[24] A new thermodynamic assessment of this system was carried out by Li et al.[25] too. According to Fütauer et al.[24] and Li et al.,[25] solid solution (Cu), $Cu_{17}Sn_3$, Cu_3Sn and liquid are stable at 700 °C in the Cu-Sn system. $Cu_{17}Sn_3$ and Cu_3Sn (ht), designated as β and γ in Ref 24 respectively, presenting order–disorder transition with composition change, are stable in the composition range of 15.0-27.5 Sn at.% at 700 °C respectively. $Cu_{17}Sn_3$ has the bcc W prototype, and Cu_3Sn (γ) adopts the fcc BiF_3 prototype.

The Zr-Sn system was experimentally updated and assessed by Pérez et al.[26] Four binary compounds were found to exist at 700 °C, i.e., $ZrSn_2$, Zr_5Sn_4, Zr_5Sn_3, and Zr_4Sn in this system.[26] Zr_5Sn_3 (Mn_5Si_3 prototype structure) and Zr_5Sn_4 (Ti_5Si_4 prototype structure) have close related crystallographic structures.[27] These two phases are stable up to 1100 °C, and merge into a single phase Zr_5Sn_{3+x}, with $0 < x < 1$, at higher temperature, due to their structural similarities.[27] The Zr_5Sn_{3+x} phase was referred as η by Pérez et al.[26]

Two isothermal sections of the Zr-Sn-Cu system at 397 and 497 °C were experimentally determined by Romaka et al. across the whole composition range.[28] Two new ternary compounds, ZrCuSn and $ZrCuSn_2$, were identified. The ZrCuSn compound adopts the TiNiSi structure type with cell parameters of $a = 0.66279(1)$ nm, $b = 0.43679(9)$ nm, $c = 0.76791(2)$ nm. The $ZrCuSn_2$ compound has the $HfCuSi_2$ structure type with cell parameters of $a = 0.41350(7)$ nm, $c = 0.9225(3)$ nm. Most commercial zirconium-based alloys are thermally fabricated, for example, by forging and extruding in the temperature range from 700 to 800 °C. In this work, the isothermal section of this system at 700 °C was investigated.

2 Experimental Procedures

Nuclear grade sponge Zr, pure Cu (99.95 wt.%), and Sn (99.95 wt.%) were used as starting materials. Ingots (4 g) were arc melted under the environment of pure argon (99.99%). To reduce contamination by oxygen, a titanium getter was melted prior to melting. The resultant buttons were sealed in vacuum quartz tubes. The alloy buttons were directly annealed at 700 °C for 60 days followed by water quench.

The alloys were subject to x-ray diffraction (XRD). The XRD was carried out on the XD-3 diffractometer with CuKa radiation and graphite monochromator. The metallographic specimens were prepared by mechanical grinding and polishing, but without etching. Microstructural observation and compositional analysis were carried out on a Scanning Electron Microscope (SEM, EVO 18) coupled with energy dispersive spectrometer (EDS, Bruke). Compositions of the alloys and those of the identified phases were obtained in area scan mode and dot scan mode, respectively, with ZAF corrections. No standard was used for the EDS compositional analysis. Chemical composition for each phase is the average of at least three measurements.

3 Results and Discussions

Results of the investigated alloys by combining use of SEM/EDS and XRD are presented in Table 1. Measured compositions for the investigated alloys and the identified phases are included. It is noted that phase identification is mainly based on composition, because of the overlap of diffraction peak in the Zr-Cu compounds.

The Zr-Sn-Cu phase diagram at 700 °C is given in Fig. 1. A new ternary compound, designated as τ, was found in this work. The previously reported ternary compounds, ZrCuSn and $ZrCuSn_2$,[28] were designated as τ_1 and τ_2 in Fig. 1, respectively. Tie-triangles with dash lines were deduced by the adjacent phase relationships and Gibbs' phase rule. The end-points of these tie-triangles were tentatively determined, too. $Cu_{17}Sn_3$ (β) and Cu_3Sn (γ) experience order–disorder transition with the composition change.[24,25] A dash line was drawn to separate two-phase region of [β + ZrCuSn] and [γ + ZrCuSn]. For the convenience of the reader, the composition points for the

Table 1 Experimental results of the Zr-Cu-Sn alloys by XRD and SEM/EDS

No.	Measured and nominal compositions(a)			Phase identified	Measured compositions		
	Zr	Cu	Sn		Zr	Cu	Sn
1	73.9	8.0	18.1	αZr	96.3	0.0	3.5
	70	10	20	Zr_5Sn_3	58.8	8.3	32.9
2	73.0	18.0	9.0	αZr	95.5	1.2	3.3
	70	20	10	Zr_5Sn_3	60.0	10.2	29.8
				$CuZr_2$	73.6	22.2	4.2
3	67.1	12.9	20.0	Zr_5Sn_3	57.8	9.3	32.9
	65	15	20	αZr	94.7	0.7	4.7
				$CuZr_2$	74.5	24.1	1.3
4	61.6	7.3	31.1	Zr_5Sn_3	58.9	6.0	35.1
	60	10	30	αZr	94.8	0.6	4.7
				$CuZr_2$	72.2	26.7	1.1
5	90.8	4.6	4.6	αZr	95.4	0.4	4.2
	90	5	5	Zr_5Sn_3	67.5	9.3	23.1
				$CuZr_2$	71.3	27.8	0.9
6(b)	52.2	25.9	21.9	Zr_5Sn_4	56.1	11.6	32.3
	50	25	25	$Cu_{10}Zr_7$	43.5	56.3	0.2
				CuZr	52.2	48.7	0.1
7(b)	56.7	25.3	18.0	Zr_5Sn_4	58.5	11.2	30.3
	55	25	20	$CuZr_2$	66.7	33.1	0.2
				CuZr	50.5	49.2	0.3
				$Cu_{10}Zr_7$		n.d.	
8(b)	62.8	28.0	9.2	Zr_5Sn_4	56.1	12.5	31.5
	60	30	10	$CuZr_2$	70.4	29.4	0.2
				CuZr	52.7	47.0	0.3
				$Cu_{10}Zr_7$		n.d.	
9(b)	52.8	38.5	8.7	Zr_5Sn_4	58.2	11.0	30.9
	50	40	10	$Cu_{10}Zr_7$	45.0	54.3	0.7
				CuZr	53.1	46.6	0.3
				Cu_2Zr		n.d.	
10	45.1	22.2	32.7	Zr_5Sn_4	58.1	7.8	34.1
	43	25	32	τ_1 (ZrCuSn)	36.2	32.6	31.3
				τ	25.9	65.4	8.7
11	37.6	16.1	46.3	Zr_5Sn_4	57.6	3.6	38.8
	35	20	45	$ZrSn_2$	33.5	1.0	65.6
				τ_1 (ZrCuSn)	36.7	30.3	33.0
12(c)	9.8	57.7	32.5	τ_1 (ZrCuSn)	34.7	33.3	32.1
	10	60	30	Cu_3Sn	0.1	74.1	25.9
				Cu_6Sn_5	1.8	53.1	45.1
				(Sn)	0.1	2.3	97.7
13(c)	8.4	48.4	43.2	τ_1 (ZrCuSn)	36.7	32.4	30.9
	10	50	40	Cu_3Sn	0.0	74.6	25.4
				Cu_6Sn_5	0.0	53.6	46.4
				(Sn)	0.0	3.0	97.0
14	21.4	46.4	32.2	τ_1(ZrCuSn)	34.3	31.2	34.4
	20	50	30	Cu_3Sn	0.1	75.3	24.6

Table 1 continued

No.	Measured and nominal compositions(a)			Phase identified	Measured compositions		
	Zr	Cu	Sn		Zr	Cu	Sn
15	32.6	48.3	19.1	Zr_5Sn_4	56.9	9.4	33.8
	30	50	20	τ_1(ZrCuSn)	34.9	31.5	33.6
				τ	24.4	67.0	8.7
16	43.0	47.2	9.8	Zr_5Sn_4	54.9	13.1	32.0
	40	50	10	Cu_8Zr_3	29.6	70.3	0.1
				$Cu_{10}Zr_7$	45.2	54.0	0.8
17	24.3	52.4	23.3	τ_1(ZrCuSn)	34.7	33.1	32.2
	20	60	20	(Cu)	0.4	96.4	3.2
18	32.1	57.6	10.3	Zr_5Sn_4	55.3	12.5	32.2
	30	60	10	$Cu_{51}Zr_{14}$	22.9	76.6	0.5
				τ	24.8	67.6	7.6
19	22.2	68.1	9.8	τ	24.4	66.7	8.9
	20	70	10	(Cu)	0.0	99.3	0.7
				τ_1 (ZrCuSn)	35.2	34.2	30.6
20	15.6	38.1	46.3	τ_1 (ZrCuSn)	35.0	31.3	33.8
	20	40	40	Cu_3Sn	0.1	72.2	27.7
21	41.5	39.8	18.7	Zr_5Sn_4	55.8	11.2	33.1
	40	40	20	$Cu_{51}Zr_{14}$	23.0	76.6	0.4
				τ	25.6	66.8	7.6
22	27.7	15.4	56.9	$ZrSn_2$	35.0	0.6	64.5
	25	25	50	τ_2($ZrCuSn_2$)	25.7	24.0	50.3
23	43.4	22.8	33.8	Zr_5Sn_4	55.7	8.5	35.7
	35	35	30	τ_1 (ZrCuSn)	34.3	33.6	32.1
				τ	26.6	63.3	10.0

(a) To save the space, the measured average and nominal composition of each alloy was included together. The composition in first row for each alloy is the measured average composition, while the second row is the nominal composition

(b) CuZr was not observed by x-ray

(c) Cu_6Sn_5, and (Sn) are the products of liquid during solidification

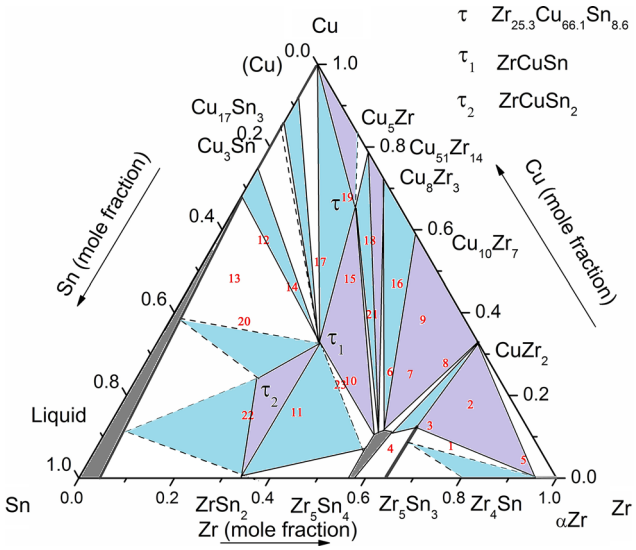

Fig. 1 Isothermal section of the Zr-Sn-Cu system at 700 °C

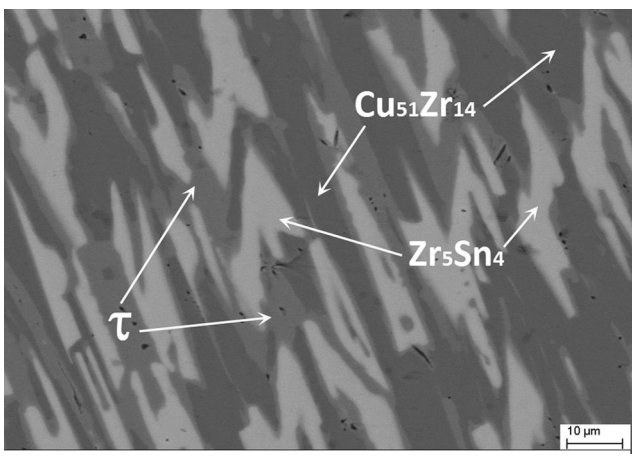

Fig. 2 BSE image of alloy 18

investigated alloys were marked in Fig. 1. It is noted that there are several composition points out of the tie-triangles defining by the alloys. As an evidence to support the existence of the related tie-triangles, results from these alloys are reserved in Table 1 too.

Figure 2 is the backscattered electron (BSE) image of alloy 18. It is clear that the alloy is composed of three phases. Composition of the white grey phase is $Zr_{55.3}Cu_{12.5}Sn_{32.2}$ (at.%), which indicates this phase is Zr_5Sn_4. The deeply grey phase $Zr_{22.9}Cu_{76.6}Sn_{0.6}$ was identified as $Cu_{51}Zr_{14}$. The composition of the grey phase is $Zr_{24.8}Cu_{67.6}Sn_{7.6}$ (at.%), designated as τ.

Alloy 21 consists of Zr_5Sn_4, $Cu_{51}Zr_{14}$, and τ phase too, as shown in Fig. 3. Results from alloys 18 and 21 indicate that the tie-triangle of (Zr_5Sn_4 + $Cu_{51}Zr_{14}$ + τ) is in this system. The τ phase with very similar composition was observed in alloys 10, 15, 19, and 23, see Table 1. The average composition of τ is calculated to be $Zr_{25.3}Cu_{66.1}Sn_{8.6}$. Co-existence of τ and $Cu_{51}Zr_{14}$ in alloys 18 and 21 reveals that τ and $Cu_{51}Zr_{14}$ are different. This τ phase is identified as a new ternary compound rather than a ternary phase derived from the nearby Zr-Cu compounds. Further work needs to be done to clarify the nature of this new ternary compound.

The tie-triangle of [(Cu) + τ + ZrCuSn] is supported by phase identification in alloy 19, as shown in Fig. 4. The dark phase with composition of $Cu_{99.3}Sn_{0.7}$ is (Cu). The grey phase with composition of $Zr_{35.2}Cu_{34.2}Sn_{30.6}$ is ZrCuSn. The white grey phase with composition of $Zr_{24.4}Cu_{66.7}Sn_{8.9}$ is the new ternary compound τ. The color contract in the BSE image is related to the average atomic number of the phase. In this alloy, (Cu) with lowest average atomic number is the darkest.

X-ray diffraction (XRD) observed major $CuZr_2$ and Zr_5Sn_4, and minor $Cu_{10}Zr_7$ in alloy 7, as shown in Fig. 5(a). Figure 5(b) is the BSE image for microstructure of this alloy. As shown in Fig. 5(b), the white grey phase with composition of $Zr_{58.5}Cu_{11.2}Sn_{30.3}$ is Zr_5Sn_4, which is confirmed by XRD. Phases between the island Zr_5Sn_4 have little color contract in the BSE image. However with the help of EDS, the deeply grey phase is CuZr with a

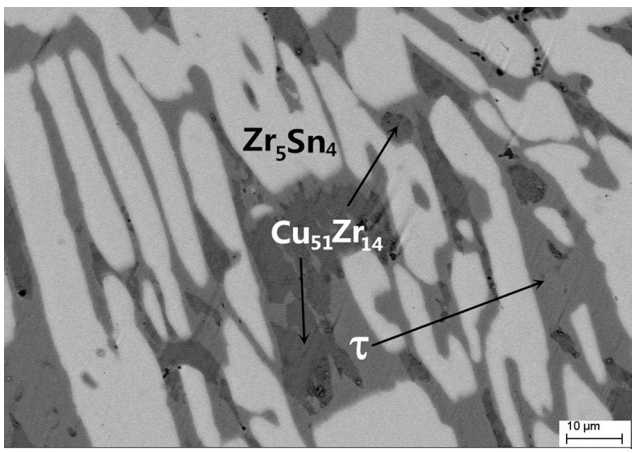

Fig. 3 Microstructure of alloy 14

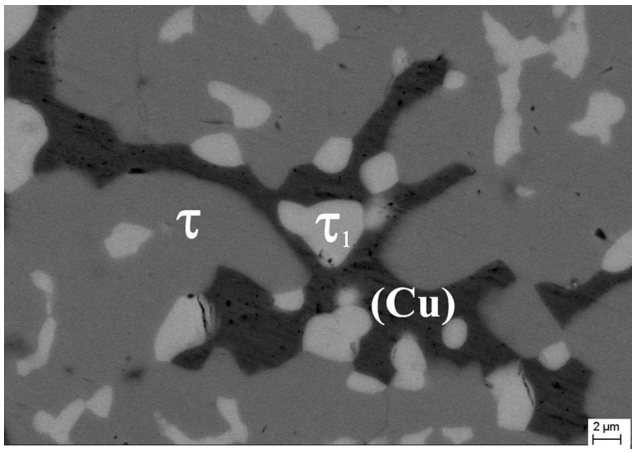

Fig. 4 BSE image of alloy 19

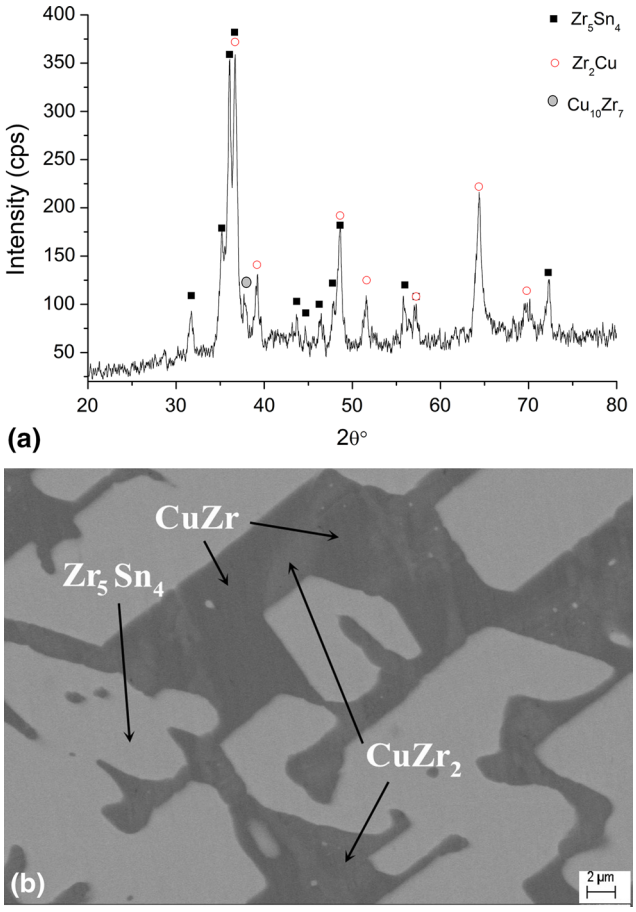

Fig. 5 (a) XRD and (b) BSE image of alloy 7. XRD detects only strong peaks of $Cu_{10}Zr_7$

measured composition to be $Zr_{50.5}Cu_{49.2}Sn_{0.3}$ and the grey phase is $CuZr_2$ with a composition of $Zr_{66.7}Cu_{33.1}Sn_{0.2}$. The boundary between CuZr and $CuZr_2$ is dim, which imply that CuZr is in the diffusion processing. The composition of $Cu_{10}Zr_7$ was not detected. Similar results were found in alloy 9, where Zr_5Sn_4 and $Cu_{10}Zr_7$ and $CuZr_2$ were detected by XRD. However, EDS detected only the composition of Zr_5Sn_4 and $Cu_{10}Zr_7$ and CuZr. The boundary between CuZr and $Cu_{10}Zr_7$ is not clear too. The CuZr phase decomposes via. eutectoid reaction $CuZr \leftrightarrow Cu_{10}Zr_7 + CuZr_2$ at 717.6 °C.[19] The dim boundary of CuZr phase and Cu_2Zr in alloy 7, and $Cu_{10}Zr_7$ in alloy 8 suggested that CuZr is in diffusion decomposition processing. Thus, CuZr phase detected in alloys 6-9 is considered to be metastable. Results in alloys 7 and 8 define the tie-triangle of [$Cu_{10}Zr_7 + Zr_5Sn_4 + CuZr_2$].

The tie-triangle of ($Zr_5Sn_4 + Cu_{10}Zr_7 + Cu_8Zr_3$) is supported by alloy 16 as seen in the Fig. 6. The white grey phase $Zr_{54.9}Cu_{13.1}Sn_{32.0}$ is Zr_5Sn_4, and the white light grey phase $Zr_{29.6}Cu_{70.3}Sn_{0.1}$ is Cu_8Zr_3, while the deeply grey phase $Zr_{45.2}Cu_{54.0}Sn_{0.8}$ is $Cu_{10}Zr_7$.

Figure 7 is the BSE image of alloy 15. The BSE image shows that the alloy consists of three phases. These phases were identified to be Zr_5Sn_4, τ, and ZrCuSn by considering the results from XRD and SEM/EDS analysis. The composition of Zr_5Sn_4 is $Zr_{56.9}Cu_{9.4}Sn_{33.8}$, and of τ and ZrCuSn are $Zr_{24.4}Cu_{67.0}Sn_{8.7}$ and $Zr_{34.9}Cu_{31.5}Sn_{33.6}$. Coexistence of Zr_5Sn_4, τ, and ZrCuSn was observed in alloy 23 too. Results from alloys 15 and 23 confirmed the tie-triangle of (Zr_5Sn_4 + τ + ZrCuSn).

At 700 °C, liquid was present in the alloys close to the Cu-Sn side. In this work, liquid phase was observed in alloys 12 and 13. Figure 8 is the BSE image of alloy 12. The large island phase is the ZrCuSn ternary compound. The grey phase is Cu_3Sn (γ) at 700 °C. As shown in Fig. 8, the light grey phase is Cu_6Sn_5, which is the product of liquid during quenching. After the precipitate of Cu_6Sn_5, the retained liquid solidified into a mixture Cu_6Sn_5 and (Sn). These two phases could not be distinguished in the current image resolution. Results from alloy 12 define a tie-triangle [Cu_3Sn + ZrCuSn + Liquid]. Since Zr has a small solubility (5 at.% at 700 °C) in liquid Sn,[26] it is believed that Zr has small solubility in Cu-Sn liquid too. Thus, the liquid point in the tie-triangle [Cu_3Sn + ZrCuSn + Liquid] is assigned to be the point in liquidus of the Cu-Sn system at 700 °C. Figure 9 is the BSE image of alloy 13. Liquid and ZrCuSn were confirmed to exist together at 700 °C. No alloys contained [ZrCuSn + $ZrCuSn_2$ + Liquid] and [Zr_2Sn + $ZrCuSn_2$ + Liquid] were found in this work. Tie-triangles [ZrCuSn + $ZrCuSn_2$ + Liquid] and [Zr_2Sn + $ZrCuSn_2$ + Liquid] are determined based on the adjacent phase relationships. The liquid points in the these two tie-triangles are arbitrary tentative.

The $ZrCuSn_2$ phase was observed to co-exist with $ZrSn_2$ in alloy 22. This result shows that $ZrCuSn_2$ is stable at 700 °C. Taking into account the data listed in Table 1, it is

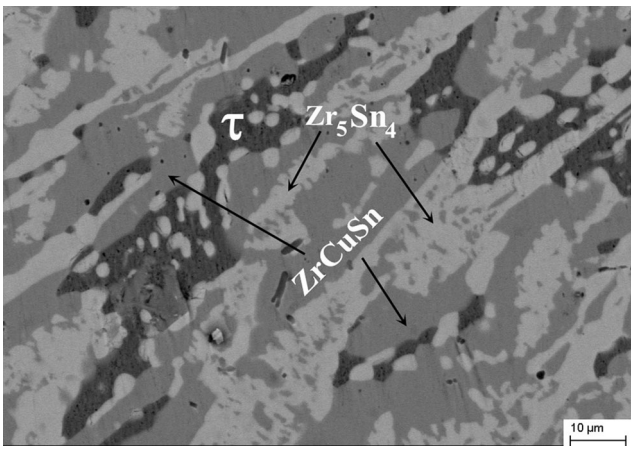

Fig. 7 BSE image of alloy 15

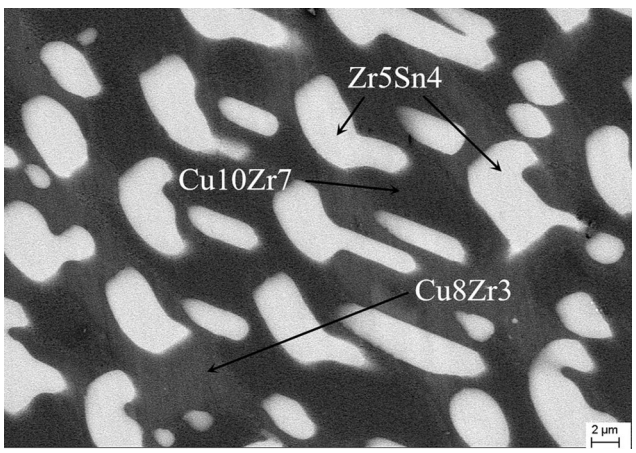

Fig. 6 Microstructure of alloy 16

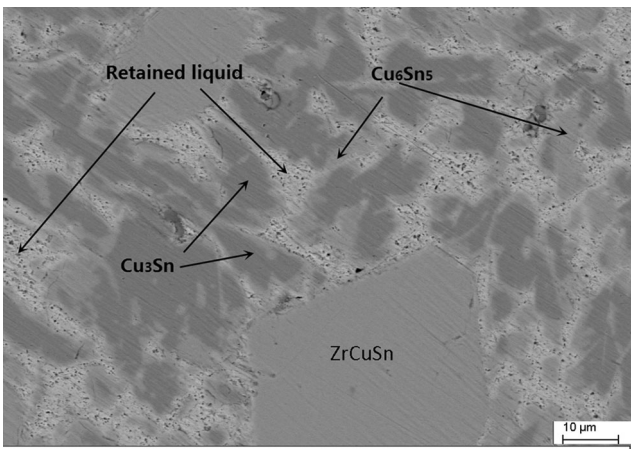

Fig. 8 BSE image of alloy 12

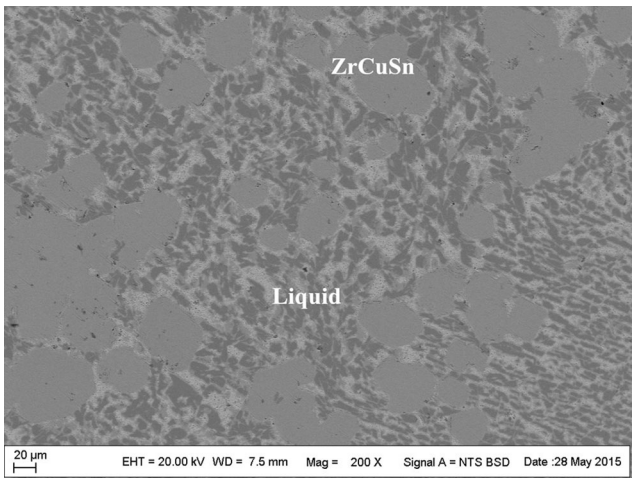

Fig. 9 BSE image of alloy 13

noted that the measured content of Sn in the Zr-Cu side binary compounds is very small. This fact means that the solubility of Sn in the Zr-Cu binary compounds is negligible.

4 Conclusions

1. A new ternary compound, designated as τ with composition of about $Zr_{25.3}Cu_{66.1}Sn_{8.6}$ was identified. The previously reported ternary compound ZrCuSn and $ZrCuSn_2$ are confirmed to be stable at 700 °C.
2. Phase relationships in the Zr-rich corner, of interested in nuclear industrial applications, are (Zr_5Sn_3 + αZr + $CuZr_2$) and (Zr_5Sn_3 + Zr_4Sn + αZr).

Acknowledgments Financial support from the Natural Science Foundation of China (51301045, 51071033), and State Nuclear Bao Ti Zirconium Industry Company are greatly appreciated.

References

1. A.J. Perry, The Properties of Directionally-Solidified Eutectic and Hypo-eutectic Copper-Zirconium Alloys, *J. Mater. Sci.*, 1973, **8**, p 443-450
2. J.A. Juarea-Islas, R. Perez, L.A. Alabarran, V. Rivera, and L. Martinz, Development of High-Strength, High-Conductivity Copper Alloys by Rapid Solidification, *J. Mater. Sci. Lett.*, 1992, **11**, p 1104-1106
3. A.T. Motta, Waterside Corrosion in Zirconium Alloys, *JOM*, 2011, **63**(8), p 63-67
4. J.M. Kim and Y.H. Jeong, Influence of Thermomechanical Treatment on the Corrosion Behavior of Zr-1Nb-0.2 Cu Alloys, *J. Nucl. Mater.*, 1999, **275**(1), p 74-80
5. H.S. Hong, J.S. Moon, S.J. Kim, and K.S. Lee, Investigation on the Oxidation Characteristics of Copper-Added Modified Zircaloy-4 Alloys in Pressurized Water at 360 °C, *J. Nucl. Mater.*, 2001, **297**(2), p 113-119
6. J.-Y. Park, B.-K. Choi, S.J. Yoo, and Y.H. Jeong, Corrosion Behavior and Oxide Properties of Zr-1.1 wt.% Nb-0.05 wt.% Cu Alloy, *J. Nucl. Mater.*, 2006, **359**(1–2), p 59-68
7. Y.H. Jeong, S.-Y. Park, M.H. Lee, B.-K. Choi, J.-H. Baek, J.-Y. Park, J.H. Kim, and H.G. Kim, Out-of-Pile and In-Pile Perfomance of Advanded Zirconium Alloys (HANA) for High Burn-Up Fuel, *J. Nucl. Sci. Technol.*, 2006, **43**(9), p 977-983
8. S. Li, M. Yao, X. Zhang, J. Geng, J. Peng, and B. Zhou, Effect of Adding Cu on the Corrosion Resistance of M5 Alloy in Superheated Steam at 500 °C, *Acta Metall. Sin.*, 2011, **47**(2), p 163-168
9. M.Y. Yao, Y. Zhang, S.L. Li, X. Zhang, J. Zhou, and B.X. Zhou, Effect of Cu Content on the Corrosion Resistance of Zr-0.80Sn-0.34Nb-0.39Fe-0.10Cr-xCu Alloy in Superheated Steam at 500 °C, *Acta Metall. Sin.*, 2011, **47**(7), p 872-876
10. X. Zhang, M.Y. Yao, Z.K. Li, J. Zhou, Q. Li, and B.X. Zhou, Corrosion Resistance of Zr-0.80Sn-0.4Nb-0.4Fe-0.10Cr-xCu Alloys in Super-Heated Steam at 400 °C, *Rare Met. Mater. Eng.*, 2013, **42**(6), p 1210-1214
11. L.M. Tu, J.L. Zhang, Q.D. Xu, M.Y. Yao, and B.X. Zhou, Corrosion Resistance of Zr-0.7Sn-1Nb-0.03Fe-xCu-xGe (x = 0, 0.05, 0.2) Alloys in Superheated Steam at 400 °C/10.3 MPa, *Rare Met. Mater. Eng.*, 2015, **44**(6), p 1391-1396
12. L. Chen, Q. Zeng, J. Li, J. Lu, Y. Zhang, L.-C. Zhang, X. Qin, W. Lu, L. Zhang, and L. Wang, Effect of Microstructure on Corrosion Behavior of a Zr-Sn-Nb-Fe-Cu-O Alloy, *Mater. Des.*, 2016, **92**, p 888-896
13. L. Chai, B. Luan, J. Chen, J. Zhou, and Q. Liu, Effect of Cooling Rate on β → α Transformation During Quenching of a Zr–0.85Sn–0.4Nb–0.4Fe–0.1Cr–0.05Cu Alloy, *Sci. China Ser. E*, 2012, **55**(10), p 2960-2964
14. L.J. Chai, B.F. Luan, S.S. Gao, J.W. Chen, and Q. Liu, Study of Precipitate Evolution and Recrystallization of Beta-Quenched Zr-Sn-Nb-Fe-Cr-Cu Alloy During Aging, *J. Nucl. Mater.*, 2012, **427**(1–3), p 274-281
15. Y. Du, S. Liu, L. Zhang, H. Xu, D. Zhao, A. Wang, and L. Zhou, An Overview on Phase Equilibria and Thermodynamic Modeling in Multicomponent Al Alloys: Focusing on the Al-Cu-Fe-Mg-Mn-Ni-Si-Zn System, *CALPHAD*, 2011, **35**(3), p 427-445
16. D. Arias and J.P. Abriata, Cu-Zr (Copper-Zirconium), *Bull. Alloys Phase Diagr.*, 1990, **11**, p 452-459
17. K.J. Zeng, M. Hamalainen, and H.L. Lukas, A New Thermodynamic Description of the Cu-Zr System, *J. Phase Equilib.*, 1994, **15**, p 577-586
18. D.H. Kang and I.H. Jung, Critical Thermodynamic Evaluation and Optimization of the Ag-Zr, Cu-Zr and Ag-Cu-Zr Systems and its Applications to Amorphous Cu-Zr-Ag Alloys, *Intermetallics*, 2010, **18**, p 815-833
19. Y. Liu, S. Liu, C. Zhang, Y. Du, J. Wang, and Y. Li, Experimental Investigation and Thermodynamic Description of the Cu-Zr System, *J. Phase Equilib. Diffus.*, 2017, **38**, p 121-134
20. M.Y.W. Lou and N.J. Grant, Identification of Cu_5Zr Phase in Cu-Zr Alloys, *Metall. Trans. A*, 1984, **15**, p 1491-1493
21. R.P. Singh, A. Lawley, S. Friedman, and Y.V. Murty, Microstructure and Properties of Spray Cast CuZr Alloys, *Mater. Sci. Eng. A*, 1991, **145**, p 243-255
22. M.A. Turchanin, P.G. Agraval, and A.R. Abdulo, Electron Microscopic Investigation of Aging in the Cu-0.06% Zr Alloy, *Phys. Met. Metall.*, 2016, **117**, p 710-718
23. L.J. Peng, X.J. Mi, B.Q. Xiong, H.F. Xie, and G.J. Huang, Microstructure of Phases in a Cu-Zr Alloy, *Rare Met.*, 2015, **34**(10), p 706-709
24. S. Fürtauer, D. Li, D. Cupid, and H. Flandorfer, The Cu-Sn Phase Diagram, Part I: New Experimental Results, *Intermetallics*, 2013, **34**, p 142-147

25. D. Li, P. Franke, S. Fürtauer, D. Cupid, and H. Flandorfer, The Cu-Sn Phase Diagram Part II: New Thermodynamic Assessment, *Intermetallics*, 2013, **34**, p 148-158
26. R.J. Pérez, C. Toffolon-Masclet, J.M. Joubert, and B. Sundman, The Zr-Sn Binary System: New Experimental Results and Thermodynamic Assessment, *CALPHAD*, 2008, **32**, p 593-601
27. Y.-U. Kwon and J.D. Corbett, The Zirconium-Tin System, with Particular Attention to the Zr_5Sn_3-Zr_5Sn_4 Region and Zr4Sn, *Chem. Mater.*, 1990, **2**, p 27-33
28. L. Romaka, N. Koblyuk, Y.V. Stadnyk, D. Frankevych, and R. Skolozdra, Phase Equilibria in the Zr-Cu-Sn System and Crystal Structure of ZrCuSn and $ZrCuSn_2$, *Pol. J. Chem.*, 1998, **72**(7), p 1154-1159